Published in final edited form as:
J Vasc Interv Radiol. 2011 December ; 22(12): 1765–1772.e1. doi:10.1016/j.jvir.2011.08.026.

Expression of profibrotic genes in the murine remnant kidney model

Binxia Yang, MD, PhD[*], **Pawan Vohra, PhD**[*], **Rajiv Janardhanan, PhD**, **Khamal D. Misra, BS**, and **Sanjay Misra, MD**

Abstract

PURPOSE—To test the hypothesis that there is increased expression of several profibrotic genes including matrix metalloproteinase–2 (MMP-2), and -9 (MMP-9), and its inhibitors (TIMP-1 and TIMP-2), a disintegrin and metalloproteinase with thrombospondin motif -1 (ADAMTS-1), and fibroblast specific protein-1 (FSP-1) in a murine remnant kidney (RK) model.

MATERIALS AND METHODS—CKD was created in ten C57BL/6 male mice (20-25 g) by performing a right nephrectomy and ligation of the upper pole of the left kidney (RK). Animals were sacrificed at 42 and 56 days later. Real time polymerase chain reaction (RT-PCR) for MMP-2, MMP-9, TIMP-1, TIMP-2, ADAMTS-1, and FSP-1 was performed in the RK. Histologic evaluation of the RK was performed using Ki-67, α-smooth muscle cell actin (α-SMA), hematoxylin and eosin, and Masson's trichrome staining. Kidney function was assessed using serum BUN and creatinine.

RESULTS—The mean serum BUN and creatinine levels at day 42 and 56 were significantly higher than baseline (P <0 .05). By day 42, the mean expression of MMP-2, MMP-9, TIMP-1, ADAMTS-1, and FSP-1 was significantly higher in the RK when compared to normal kidney ($P<0.05$) and by day 56, only FSP-1 expression increased significantly higher ($P<0.05$). There was increased fibrosis by Masson's trichrome, increased Ki-67, with increased α-SMA staining in the RK when compared to normal kidneys.

CONCLUSIONS—In the RK, there was increased fibrosis with increased α -SMA and Ki-67 staining with significantly increased expression of MMP-2, MMP-9, TIMP-1, ADAMTS-1, and FSP-1.

Introduction

In the United States, it is estimated that more than 20 million people are affected with chronic kidney disease affects (1). This population will increase because of the rising prevalence of the etiologies of chronic kidney disease, including diabetes, hypertension, and obesity (2-6). Patients with chronic kidney disease have increased cardiovascular complication rates as well as acute and chronic renal failure requiring renal replacement

Correspondence: Sanjay Misra, MD FSIR, FAHA, Associate Professor, Mayo Clinic, 200 First Street SW, Department of Radiology, Division of Vascular and Interventional Radiology, Vascular and Interventional Translational Lab, Rochester, MN 55902, Telephone: 507-255-7208, Fax: 507-255-7872, misra.sanjay@mayo.edu.
[*]Both authors contributed equally to this manuscript.

therapy (7). Understanding the mechanisms responsible for chronic kidney disease is important so that therapies could be developed that improve clinical outcomes in patients.

Histologic evaluation of kidneys removed from patients with chronic kidney disease demonstrate changes consistent with angiogenesis and inflammation accompanied with glomerulosclerosis and tubular interstitial fibrosis which is felt to contribute to the decline in kidney function (8). It has been hypothesized that these histologic changes are caused by changes in angiogenic and matrix regulatory proteins including vascular endothelial growth factor-A (VEGF-A), matrix metalloproteinase (MMPs), a disintegrin and metalloproteinase with thrombospondin motif -1 (ADAMTS-1), and others (9-16). Each of these proteins has been found to be increased in experimental animal models and in patients with chronic kidney disease.

In order to determine the mechanisms of chronic kidney disease, animal models have been created in which one kidney is removed along with half of the contralateral kidney known as the remnant kidney model. Many different animals have been used for this model including rats, mice, rabbits, cats, dogs, baboons, and pigs (17-24). The purpose of the current report was to determine the expression pattern of a disintegrin and metalloproteinase with thrombospondin motif-1 (ADAMTS-1), MMP-2, MMP-9, and its inhibitors along with fibroblast specific protein-1 (FSP-1) in a murine remnant kidney model. We used C57BL/6 mice as they are resistant to fibrosis and detonation of kidney function, which occurs in the FVB mice (25, 26). The histologic changes in the remnant kidney were characterized.

Materials and Methods

Study Design

Appropriate Institutional Animal Care and Use Committee approval was obtained prior to performing any procedures. The housing and handling of the animals was performed in accordance with the Public Health Service Policy on Humane Care and Use of Laboratory Animals revised in 2000 (27). Animals were allowed access to water and food ad libitum. Anesthesia was achieved with intraperitoneal injection of a mixture of ketamine hydrochloride (0.20 mg/g) and xylazine (0.02 mg/g) and maintained with intraperitoneal pentobarbital (20-40 mg/kg). Ten male C57BL/6 mice (Jackson Laboratories, Bar Harbor, ME) weighing 25-30 grams were used for the present study. Chronic renal insufficiency was created by surgical removal of the right kidney accompanied by ligation of the arterial blood supply to the upper pole of the left kidney as described previously (28). The right kidney was used for comparison and designated as normal kidney for the PCR and histologic analyses. The right kidney was weighed after removal. Serum BUN and creatinine were measured by removing blood from the tail vein at baseline (before nephrectomy) and at the time of sacrifice. The animals were sacrificed at day 42 (n=5) and 56 (n=5) later. The animals were weighed weekly after the nephrectomy.

Tissue harvesting

At euthanasia, all mice were anesthetized as described previously and euthanized by CO_2 asphyxiation and the remnant kidney harvested for RT-PCR, histologic, or protein analyses as described previously (28, 29). The RK was removed and weighed as previously described (28).

RNA isolation

The tissue was stored in RNA stabilizing reagent (Qiagen, Gaithersburg, MD) as per the manufactures guidelines. To isolate the RNA, the specimens were homogenized and total RNA isolated using RNeasy mini kit (Qiagen) (28, 29).

Real time polymerase chain reaction (RT-PCR) analysis

Expression for the genes of interest was determined using RT-PCR analysis (29). Briefly, first-strand complementary DNA (cDNA) was synthesized using superscript III first strand (Invitrogen, Carlsbad, CA) according to the manufacturer's guidelines. cDNAs specific for the genes analyzed were amplified using primers described in Table 1 (28). PCR products were analyzed on 1.5% (w/v) agarose gels containing 0.5-μg/ml ethidium bromide. Bands were quantified by scanning densitometry (Image J version 1.43, NIH, Bethesda, MD). An area of the gel image that was devoid of signal was assigned to be the background value. Then each band representing the gene of interest was analyzed for the density above background. Next, it was normalized to the amount of loading of mRNA to 18S gene to ensure that there were no differences in loading and then pooled for all the animals in the different treatment groups for each time period.

Immunohistochemistry

Hematoxylin and eosin, Masson's trichrome, Ki-67, and α-SMA staining were performed on 5-μm thick paraffin embedded sections from the remnant kidney or control kidney using the Vectastain Elite ABC system (Vector Laboratories, Burlingame, CA, USA) as described previously (30, 31). The following antibodies were used: mouse monoclonal antibody Ki-67 (DAKO, Carpentaria, CA; 1:400) or rabbit polyclonal antibody to mouse for α-SMA (Abcam, Cambridge, MA; 1:400).

Statistical methods

Data are expressed as mean ± SEM. Two groups were compared with 2-tailed unpaired Student's t-test. Significant difference from control value was indicated by $*P < 0.05$. SAS version 9 (SAS Institute Inc., Cary, N.C.) was used for statistical analyses.

Results

Surgical outcomes

The mean body weight of the mouse at baseline was 23.2 ± 2.2 g and decreased to 20 ± 3.2 g by 7 days after nephrectomy when compared to weight at the time of nephrectomy ($P<0.05$). By day 28, the average weight had increased to 23 ± 3.2 g and by days 42 to 56, it had increased to 25 ± 2.2 ($P = NS$). The right kidney at nephrectomy weighed 150 ± 15 mg. By day 42, the average weight of the remnant kidney had increased to 180 ± 10 mg and by day 56, it was 178 ± 5 mg ($P<0.05$ for both time points when compared to the right kidney).

Serum BUN and creatinine changes after nephrectomy

The mean BUN and creatinine at baseline was 28 ± 5 mg/dL and 0.24 ± 0.1 mg/dL, respectively. The mean serum BUN increased significantly by day 42 (49 ± 7.8 mg/dL) and continued to rise by day 56 (60 ± 4.8 mg/dL) when compared to baseline ($P<0.05$). The mean serum creatinine increased significantly by day 42 (0.34 ± 0.01 mg/dL) and remained significantly elevated by day 56 (0.42 ± 0.1 mg/dL) when compared to baseline ($P<0.05$). These data indicate that the mice had developed chronic renal insufficiency at day 42 and 56 after nephrectomy.

Hematoxylin and eosin with Masson's trichrome staining in the remnant kidney at day 42 and 56

We assessed the histologic changes in the remnant kidney by performing hematoxylin and eosin (H and E) staining on representative sections removed from the normal kidney (column one) and the remnant kidney from day 42 and 56 after nephrectomy as shown in figure 1. The H and E staining showed increased cellular localization in the tubular

interstitial compartment (yellow arrows). We next assessed fibrosis by performing Masson's trichrome staining on representative sections removed from the normal kidney (column one) and the remnant kidney from day 42 and 56 after nephrectomy as shown in figure 2. Compared to the normal removed kidneys, there was an accumulation of fibrotic tissue (blue stain, yellow arrows) in the tubular interstitial compartment of the remnant kidneys on day 42, with even greater staining on day 56. These changes are consistent with the clinical scenario.

Ki-67 staining in the remnant kidney at day 42 and 56

Because there was increased fibrosis and cellular density, we assessed whether this was due to an increase in cellular proliferation using Ki-67 staining which is a nuclear stain (yellow arrow) on representative sections removed from the normal kidney (column one) and the remnant kidney from day 42 and 56 after nephrectomy as shown in figure 3. Cells staining positive for Ki-67 have brown colored nuclei. The normal kidney shows no evidence of Ki-67 positive cells while there is increased staining for Ki-67 positive cells by day 42 and 56. Overall, these results indicate that there is increased proliferation in the remnant kidney by days 42 and 56.

a-SMA staining in the remnant kidney at day 42 and 56

Finally, we assessed the increase in smooth muscle cell density by staining for α-smooth muscle actin (α-SMA) on representative sections removed from the normal kidney (column one) and the remnant kidney from day 42 and 56 after nephrectomy as shown in figure 4. Cells staining positive for α -SMA are brown (yellow arrow). The normal kidney shows no evidence of α-SMA positive cells while there is increased staining for cells staining brown by day 42 and 56. Overall, these results indicate that there are increased cells staining positive for α-SMA in the remnant kidney by days 42 and 56 localized to the tubulo-interstitial compartment.

Gene expression of MMP-2 and MMP-9 in the remnant kidney at day 42 and 56

Increased expression of MMP-2 has been shown in the remnant kidney model (16, 32). We assessed MMP-2 (Fig. 5) and MMP-9 expression (Fig. 6) by RT-PCR performed in the normal and remnant kidney at day 42 and 56 after nephrectomy. By day 42, the mean expression of both MMP-2 and MMP-9 in remnant kidney was significantly higher (3.32 ± 0.13 and 3.99 ± 0.2, respectively) when compared to the control kidney (1.6 ± 0.013 and 1.17 ± 0.13, respectively $P<0.05$). By day 56, the mean gene expression for both MMP-2 and MMP-9 had significantly decreased in the remnant kidney when compared to the control. Overall, these results indicate that there is increased expression of MMP-2 and MMP-9 in the remnant kidney by days 42 which decreases by day 56.

Gene expression of TIMP-1 and TIMP-2 in the remnant kidney at day 42 and 56

We assessed the changes in TIMP-1 and TIMP-2 expression using RT-PCR in the control and remnant kidney at day 42 and 56. By day 42, the mean expression of TIMP-1 was significantly higher (3.5 ± 0.13) when compared to the control kidney (0.3 ± 0.05, $P<0.05$) (Fig. 7). By day 56, the mean gene expression for both TIMP-1 had significantly decreased in the remnant kidney when compared to the control. In contrast, the mean expression of TIMP-2 at day 42 was the same as control and decreased significantly by day 56 when compared to control.

Gene expression of ADAMTS-1 in the remnant kidney at day 42 and 56

ADAMTS-1 is an inhibitor of VEGF-A and has been shown to be increased in the remnant kidney (16, 32). We assessed the changes in ADAMTS-1 expression using RT-PCR in the

control and remnant kidney at day 42 and 56 (Fig. 8). By day 42, the mean expression of ADAMTS-1 in the remnant kidney was significantly higher (0.22 ± 0.02) when compared to the control kidney (0.11 ± 0.01, $P<0.05$). By day 56, the mean gene expression for ADAMTS-1 had returned to normal in the remnant kidney when compared to the control. Overall, these results indicate that there is increased expression of ADAMTS-1 by day 42 that normalizes by day 56.

Gene expression of FSP-1 in the remnant kidney at day 42 and 56

Since there was increased fibrosis by Masson's trichrome with increased α-SMA staining in the remnant kidney, we assessed these changes using fibroblast specific factor-1 which is a marker for α-SMA using RT-PCR in the remnant kidney and control kidneys at day 42 and 56 (Fig. 9). By day 42, the mean expression of FSP-1 in the remnant kidney was significantly higher (1 ± 0.05) when compared to the control kidney (0.74 ± 0.05, $P<0.05$). By day 56, the mean gene expression for FSP-1 continued to increase (2.01 ± 0.11, $P<0.05$) significantly in the remnant kidney when compared to the control.

Discussion

Understanding the mechanisms of chronic kidney disease is important in developing and selecting therapies that will improve health care outcomes. In the present paper, we determined the gene expression of several important profibrotic genes including MMP-2, MMP-9, TIMP-1, TIMP-2, ADAMTS-1, and FSP-1 in the murine remnant kidney. We found that there is increased gene expression of MMP-2, MMP-9, TIMP-1, ADAMTS-1, and FSP-1 at day 42 with continued expression of FSP-1 at day 56. We observed that the remnant kidney undergoes compensatory enlargement by increasing the kidney weight with tubular interstitial fibrosis and scarring that worsens over time. Finally, we observed increased cellular proliferation with smooth muscle density in the remnant kidney when compared to control.

Many different remnant kidney animal models have been used to study the mechanism of chronic kidney disease (17-24). We used the murine model of chronic kidney disease to determine the changes in several important profibrotic genes. The major advantage of the murine model is that it enables the use of genetically altered mice to determine the significance of these genes in chronic kidney disease. In the present study, the mice had a significant increase in BUN and creatinine levels at day 42 and 56 after nephrectomy. The remnant kidney exhibits compensatory enlargement with tubular interstitial fibrosis and scarring by day 42 and 56 after nephrectomy.

There have been several hypotheses to explain the mechanisms of chronic kidney disease. These include increased expression of proteins involved in inflammation, angiogenesis, and extracellular matrix deposition (13, 15, 33, 34). Matrix metalloproteinase (MMPs) are a family of extracellular matrix degrading proteinases. Several have linked aberrant MMP and/or TIMP expression to a number of renal pathophysiology, both acute and chronic (13). The development of progressive renal failure is mainly attributed to the formation of extensive glomerular and tubular interstitial fibrosis (35). Tubular interstitial fibrosis is characterized by the accumulation of mesangial matrix and fibrosis of the glomerular basement membrane. The main constituent of the mesangial matrix and fibrosis of the glomerular and tubular basement membrane is type IV collagen that is degraded by MMP-2 and MMP-9. The degradation of this collagen is mainly inhibited by TIMP-1 (36). The results of present study shown that there is a significant increase in the expression of MMP-2, MMP-9, and TIMP-1 by day 42, which decreases, by day 56 after nephrectomy. In addition, the mean expression of TIMP-2 is significantly reduced by day 56. We suggest the

MMP-2, MMP-9 contribute the formation of remnant kidney fibrosis and these results are similar to those observed by other investigators (34).

ADAMTS-1 is a soluble MMP that can inhibit VEGF-A (37). There have been several studies, which have demonstrated involvement of VEGF-A in chronic kidney disease, diabetic nephropathy, glomerulosclerosis, and the remnant kidney model (15, 33, 34). Furthermore, inhibiting VEGF-A function using angiostatin has shown to decrease extracellular matrix deposition in the rat remnant kidney model (14). Recently, in a rat kidney model of ischemia reperfusion injury, ADAMTS-1 was increased at early time points after ischemia reperfusion while VEGF-A expression was decreased with ADAMTS-1 being localized to the proximal tubules (16). In the present study, we observed a significant increase in the average gene expression of ADAMTS-1 by day 42. The identification of ADAMTS-1 being elevated in chronic kidney disease is consistent with a study by Rumberger et al (34). In this study, nephrectomy was created in C57BL/6 mice and gene array technology was used to identify increases in ADAMTS-1 and ADAMTS-4.

In order to explore the molecular basis for the increased expression of α-SMA and fibrosis as observed histologically, we examined fibroblast specific protein-1, which is a marker for α-SMA (38, 39). The mean gene expression of FSP-1 was significantly increased by days 42 and 56 in the remnant kidney when compared to the control kidneys. This is coupled by the observation that we observed increased α-SMA staining and fibrosis in the remnant kidney. In view of these considerations, we suggest that the temporal changes in FSP-1 expression may contribute, at least in part, to the fibrotic profile observed in the remnant kidneys.

The mouse strain (C57BL/6) used in this study is known to be resistant against deterioration of kidney function after nephrectomy (25, 26). The FVB mouse in the same setting has been shown to undergo continued decline in kidney function with a majority of animals dying at three months after nephrectomy (25, 26). We chose the C57BL/6 mice because they did not have the increased mortality observed with the FVB mice (25, 26). It is possible that some of the results observed in this study could be as a result of these genetic differences.

In summary, we observed several important features in the mouse model of chronic kidney disease. There was increased mean BUN and creatinine by days 42 and 56 after nephrectomy with increased fibrosis and α-SMA staining in the remnant kidney. In addition, we observed increased gene expression of several profibrotic genes including MMP-2, MMP-9, TIMP-1, ADAMTS-1, and FSP-1. Therapeutic manipulation of these genes using knockout models will help gain further understanding of these genes in chronic kidney disease and help develop therapies, which can reduce the progression of chronic kidney disease.

References

1. Coresh J, Selvin E, Stevens LA, et al. Prevalence of chronic kidney disease in the United States. Jama. 2007; 298:2038–2047. [PubMed: 17986697]
2. Gregg EW, Cheng YJ, Cadwell BL, et al. Secular trends in cardiovascular disease risk factors according to body mass index in US adults. Jama. 2005 Apr 20.293:1868–1874. [PubMed: 15840861]
3. Fields LE, Burt VL, Cutler JA, Hughes J, Roccella EJ, Sorlie P. The burden of adult hypertension in the United States 1999 to 2000: a rising tide. Hypertension. 2004; 44:398–404. [PubMed: 15326093]
4. Hajjar I, Kotchen TA. Trends in prevalence, awareness, treatment, and control of hypertension in the United States, 1988-2000. Jama. 2003; 290:199–206. [PubMed: 12851274]
5. Mokdad AH, Ford ES, Bowman BA, et al. Prevalence of obesity, diabetes, and obesity-related health risk factors, 2001. Jama. 2003; 289:76–79. [PubMed: 12503980]

6. US Renal Data Systems. USRDS 2006 Annual Data Report: Atlas of End-Stage Renal Disease in the United States. Bethesda, MD: National Institutes of Health, National Institute of Diabetes and Digestive and Kidney Diseases; 2007.
7. Hsu CY, Ordonez JD, Chertow GM, Fan D, McCulloch CE, Go AS. The risk of acute renal failure in patients with chronic kidney disease. Kidney Int. 2008; 74:101–107. [PubMed: 18385668]
8. Fogo AB. Mechanisms of progression of chronic kidney disease. Pediatr Nephrol. 2007; 22:2011–2022. [PubMed: 17647026]
9. Ronco P, Lelongt B, Piedagnel R, Chatziantoniou C. Matrix metalloproteinases in kidney disease progression and repair: a case of flipping the coin. Semin Nephrol. 2007; 27:352–362. [PubMed: 17533011]
10. Norman JT, Gatti L, Wilson PD, Lewis M. Matrix metalloproteinases and tissue inhibitor of matrix metalloproteinases expression by tubular epithelia and interstitial fibroblasts in the normal kidney and in fibrosis. Exp Nephrol. 1995; 3:88–89. [PubMed: 7773643]
11. Norman JT, Lewis MP. Matrix metalloproteinases (MMPs) in renal fibrosis. Kidney Int Suppl. 1996; 54:S61–S63. [PubMed: 8731197]
12. Johnson TS, Haylor JL, Thomas GL, Fisher M, El Nahas AM. Matrix metalloproteinases and their inhibitions in experimental renal scarring. Exp Nephrol. 2002; 10:182–195. [PubMed: 12053120]
13. Ahmed AK, Haylor JL, El Nahas AM, Johnson TS. Localization of matrix metalloproteinases and their inhibitors in experimental progressive kidney scarring. Kidney Int. 2007; 71:755–763. [PubMed: 17290295]
14. Mu W, Long DA, Ouyang X, et al. Angiostatin overexpression is associated with an improvement in chronic kidney injury by an anti-inflammatory mechanism. Am J Physiol Renal Physiol. 2009; 296:F145–F152. [PubMed: 18971211]
15. Schrijvers BF, Flyvbjerg A, De Vriese AS. The role of vascular endothelial growth factor (VEGF) in renal pathophysiology. Kidney Int. 2004; 65:2003–2017. [PubMed: 15149314]
16. Basile DP, Fredrich K, Chelladurai B, Leonard EC, Parrish AR. Renal ischemia reperfusion inhibits VEGF expression and induces ADAMTS-1, a novel VEGF inhibitor. Am J Physiol Renal Physiol. 2008 Apr.294:F928–F936. [PubMed: 18272597]
17. Heifets M, Morrissey JJ, Purkerson ML, Morrison AR, Klahr S. Effect of dietary lipids on renal function in rats with subtotal nephrectomy. Kidney Int. 1987; 32:335–341. [PubMed: 3669493]
18. Sigmon DH, Gonzalez-Feldman E, Cavasin MA, Potter DL, Beierwaltes WH. Role of nitric oxide in the renal hemodynamic response to unilateral nephrectomy. J Am Soc Nephrol. 2004; 15:1413–1420. [PubMed: 15153552]
19. Kren S, Hostetter TH. The course of the remnant kidney model in mice. Kidney Int. 1999; 56:333–337. [PubMed: 10411710]
20. Fine LG, Trizna W, Bourgoignie JJ, Bricker NS. Functional profile of the isolated uremic nephron. Role of compensatory hypertrophy in the control of fluid reabsorption by the proximal straight tubule. The Journal of clinical investigation. 1978; 61:1508–1518. [PubMed: 659612]
21. Fine LG, Schlondorff D, Trizna W, Gilbert RM, Bricker NS. Functional profile of the isolated uremic nephron. Impaired water permeability and adenylate cyclase responsiveness of the cortical collecting tubule to vasopressin. The Journal of clinical investigation. 1978; 61:1519–1527. [PubMed: 207738]
22. Fine LG, Yanagawa N, Schultze RG, Tuck M, Trizna W. Functional profile of the isolated uremic nephron: potassium adaptation in the rabbit cortical collecting tubule. The Journal of clinical investigation. 1979; 64:1033–1043. [PubMed: 225350]
23. Adams LG, Polzin DJ, Osborne CA, O'Brien TD, Hostetter TH. Influence of dietary protein/calorie intake on renal morphology and function in cats with 5/6 nephrectomy. Lab Invest. 1994; 70:347–357. [PubMed: 8145529]
24. Misra S, Fu AA, Misra KD, Glockner JF, Mukhopadyay D. Evolution of shear stress, protein expression, and vessel area in an animal model of arterial dilatation in hemodialysis grafts. J Vasc Interv Radiol. 2010; 21:108–115. [PubMed: 20123196]
25. Ma LJ, Fogo AB. Model of robust induction of glomerulosclerosis in mice: importance of genetic background. Kidney Int. 2003; 64:350–355. [PubMed: 12787428]

26. Pillebout E, Burtin M, Yuan HT, et al. Proliferation and remodeling of the peritubular microcirculation after nephron reduction: association with the progression of renal lesions. Am J Pathol. 2001; 159:547–560. [PubMed: 11485913]
27. Committee on care and use of laboratory animals of the institute of laboratory animal resources. Washington, DC: Government print office; 1996.
28. Misra S, Shergill U, Yang B, Janardhanan R, Misra KD. Increased expression of HIF-1alpha, VEGF-A and its receptors, MMP-2, TIMP-1, and ADAMTS-1 at the venous stenosis of arteriovenous fistula in a mouse model with renal insufficiency. J Vasc Interv Radiol. 2010; 21:1255–1261. [PubMed: 20598569]
29. Yang B, Shergill U, Fu AA, Knudsen B, Misra S. The mouse arteriovenous fistula model. J Vasc Interv Radiol. 2009; 20:946–50. [PubMed: 19555889]
30. Misra S, Doherty MG, Woodrum D, et al. Adventitial remodeling with increased matrix metalloproteinase-2 activity in a porcine arteriovenous polytetrafluoroethylene grafts. Kidney Int. 2005; 68:2890–2900. [PubMed: 16316367]
31. Misra S, Fu AA, Puggioni A, et al. Increased shear stress with up regulation of VEGF-A and its receptors and MMP-2, MMP-9, and TIMP-1 in venous stenosis of hemodialysis grafts. Am J Physiol Heart Circ Physiol. 2008; 294:H2219–H2230. [PubMed: 18326810]
32. Nakamura A, Sakai Y, Ohata C, Komurasaki T. Expression and significance of a disintegrin and metalloproteinase with thrombospondin motifs (ADAMTS)-1 in an animal model of renal interstitial fibrosis induced by unilateral ureteral obstruction. Exp Toxicol Pathol. 2007; 59:1–7. [PubMed: 17583485]
33. Misra S, Misra KD, Glockner JF. Vascular endothelial growth factor-A, matrix metalloproteinase-1, and macrophage migration inhibition factor changes in the porcine remnant kidney model: evaluation by magnetic resonance imaging. J Vasc Interv Radiol. 2010; 21:1071–1077. [PubMed: 20610182]
34. Rumberger B, Vonend O, Kreutz C, Wilpert J, Donauer J, Amann K, et al. cDNA microarray analysis of adaptive changes after renal ablation in a sclerosis-resistant mouse strain. Kidney Blood Press Res. 2007; 30:377–387. [PubMed: 17890868]
35. Nath KA. Tubulointerstitial changes as a major determinant in the progression of renal damage. Am J Kidney Dis. 1992; 20:1–17. [PubMed: 1621674]
36. Akira S, Takeda K, Kaisho T. Toll-like receptors: critical proteins linking innate and acquired immunity. Nat Immunol. 2001; 2:675–680. [PubMed: 11477402]
37. Lee S, Jilani SM, Nikolova GV, Carpizo D, Iruela-Arispe ML. Processing of VEGF-A by matrix metalloproteinases regulates bioavailability and vascular patterning in tumors. J Cell Biol. 2005; 169:681–691. [PubMed: 15911882]
38. Iwano M, Plieth D, Danoff TM, Xue C, Okada H, Neilson EG. Evidence that fibroblasts derive from epithelium during tissue fibrosis. The Journal of clinical investigation. 2002; 110:341–350. [PubMed: 12163453]
39. Kalluri R, Neilson EG. Epithelial-mesenchymal transition and its implications for fibrosis. The Journal of clinical investigation. 2003; 112:1776–1784. [PubMed: 14679171]

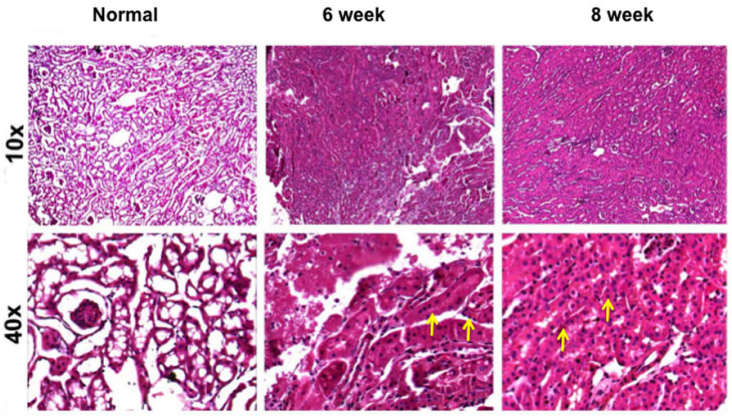

Fig. 1.

Hematoxylin and eosin (H and E) staining on representative sections removed from the normal kidney (column one) and the remnant kidney from day 42 and 56 after nephrectomy. Upper row is 10X and lower row is 40X. There is increased cellular localization in the tubular interstitial compartment (yellow arrows).

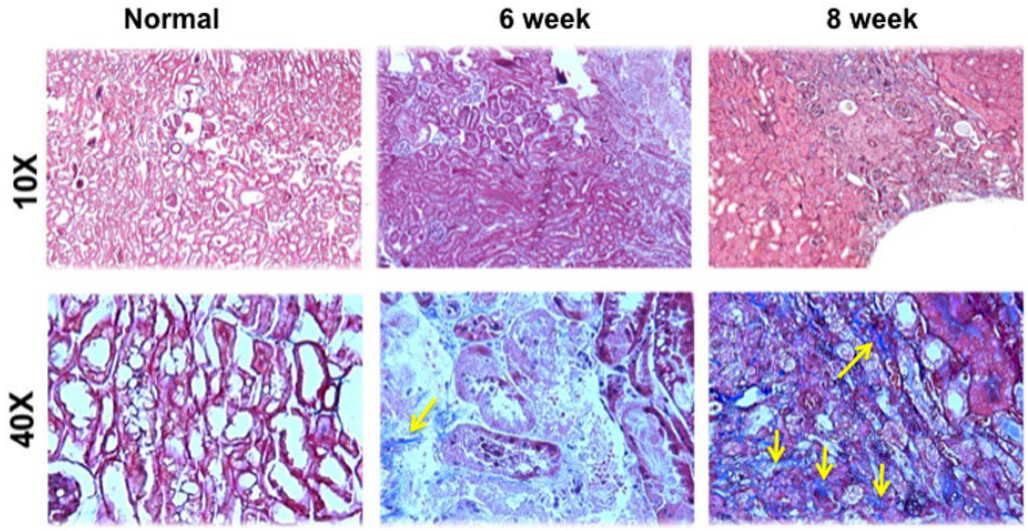

Fig. 2.

Masson's trichrome staining on representative sections removed from the normal kidney (column one) and the remnant kidney from day 42 and 56 after nephrectomy. Upper row is 10X and lower row is 40X. The normal kidney remains unaltered, while there is accumulation of fibrotic tissue (blue, yellow arrows) in the tubular interstitial compartment, which is present on day 42, and worsens by day 56 in the remnant kidney.

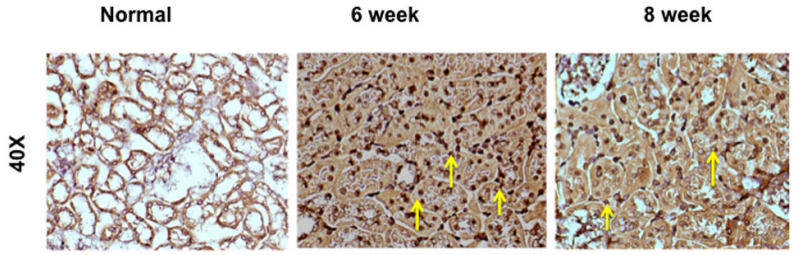

Fig. 3.

Ki-67 staining on representative sections removed from the normal kidney (column one) and the remnant kidney from day 42 and 56 after nephrectomy. Upper row is 10X and lower row is 40X. Cells staining positive for Ki-67 have brown colored nuclei. The normal kidney shows no evidence of Ki-67 positive cells while there is increased staining for Ki-67 positive cells by day 42 and 56.

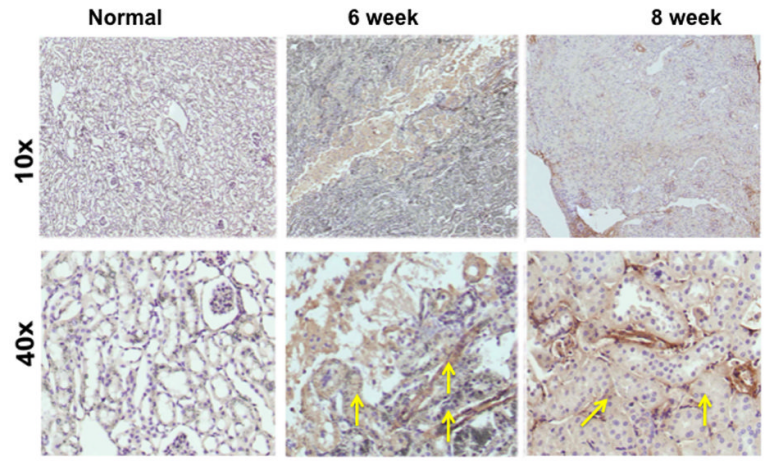

Fig. 4.

α-smooth muscle actin staining on representative sections removed from the normal kidney (column one) and the remnant kidney from day 42 and 56 after nephrectomy. Upper row is 10X and lower row is 40X. Cells staining positive for α -SMA are brown (yellow arrow). The normal kidney shows no evidence of α-SMA positive cells while there is increased staining for cells staining brown by day 42 and 56.

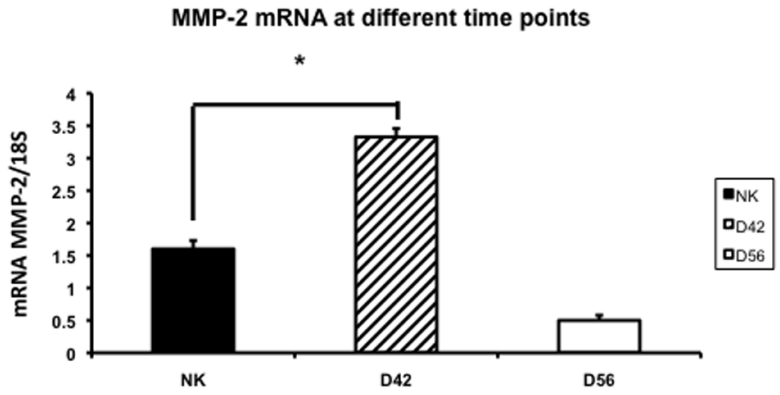

Fig. 5.

Average gene expression of matrix metalloproteinase-2 (MMP-2) in the remnant kidney at day 42 and 56 after nephrectomy. Data are mean ± SEM. (*) is $P<0.05$.

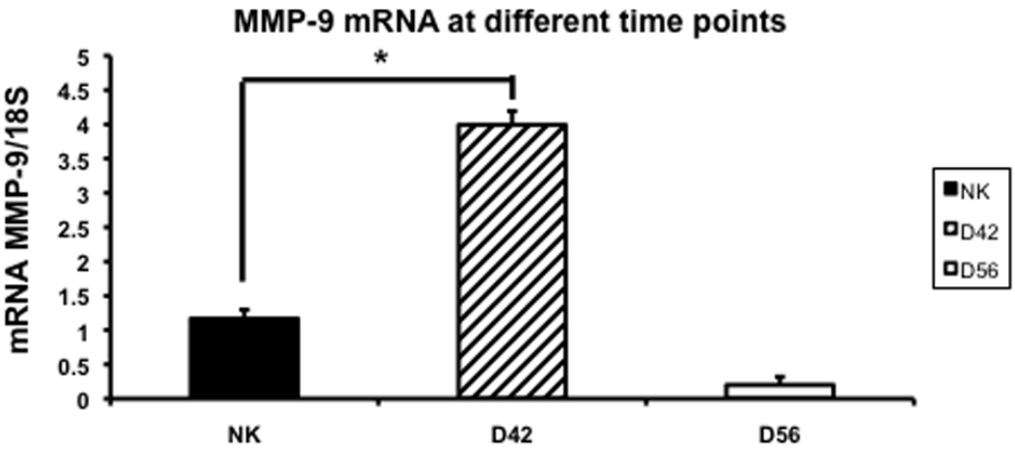

Fig. 6.

Average gene expression of matrix metalloproteinase-9 (MMP-9) in the remnant kidney at day 42 and 56 after nephrectomy. Data are mean ± SEM. (*) is $P<0.05$.

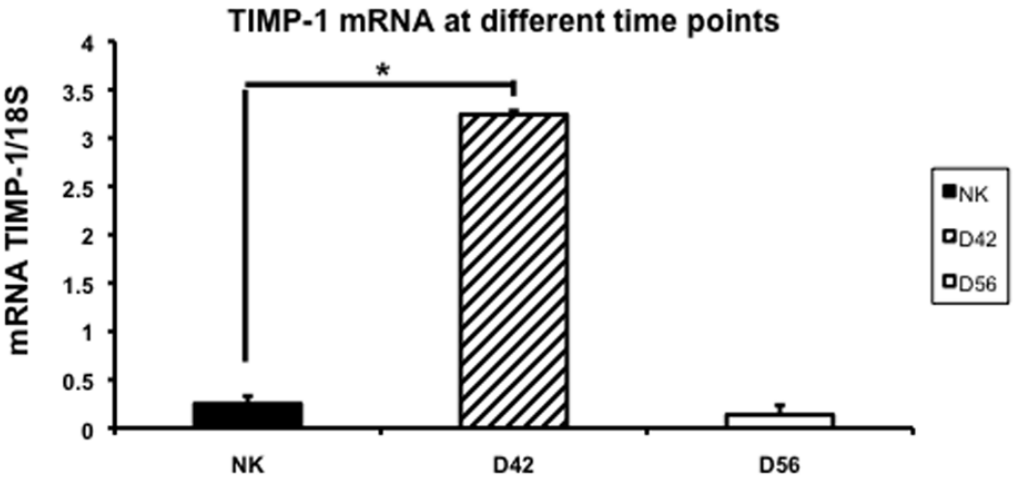

Fig. 7.

Average gene expression of tissue inhibitor of matrix metalloproteinase-1 (TIMP-1) in the remnant kidney at day 42 and 56 after nephrectomy. Data are mean ± SEM. (*) is $P<0.05$.

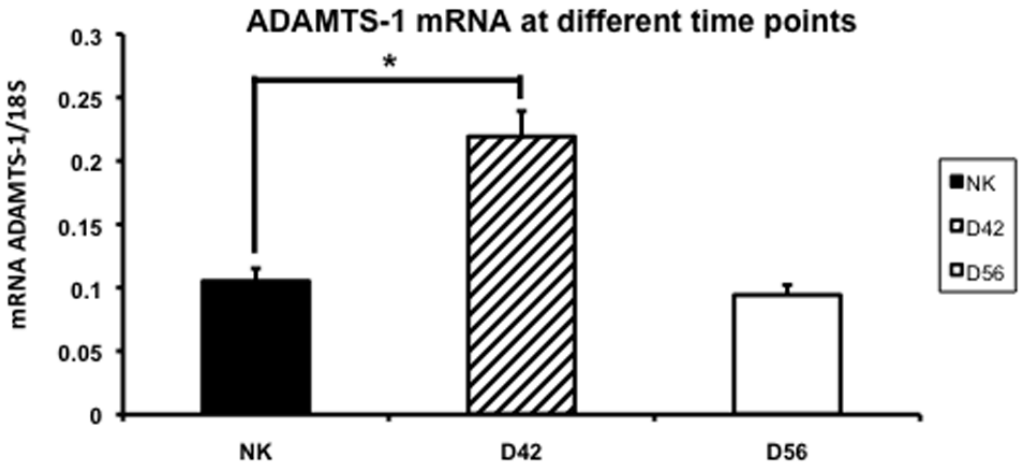

Fig. 8.

Average gene expression of a disintegrin and metalloproteinase with thrombospondin motif-1 (ADAMTS-1) in the remnant kidney at day 42 and 56 after nephrectomy. Data are mean ± SEM. (*) is $P<0.05$.

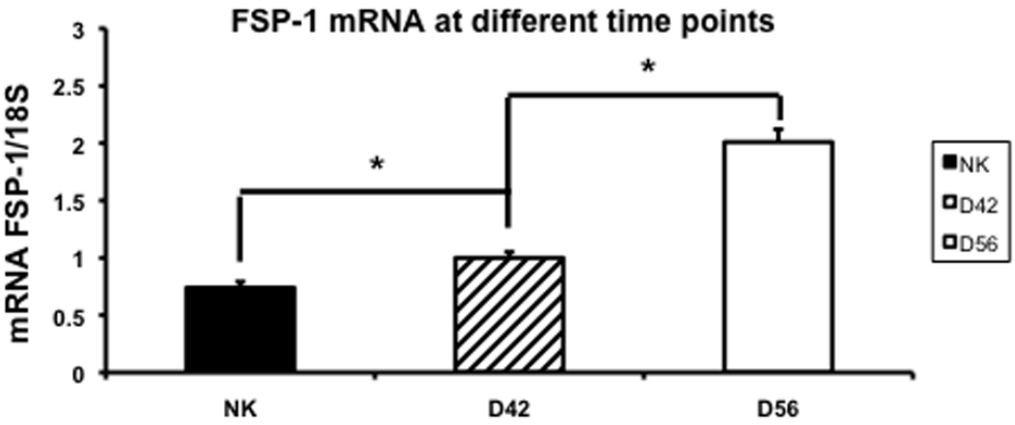

Fig. 9.

Average gene expression of fibroblast specific protein-1 (FSP-1) in the remnant kidney at day 42 and 56 after nephrectomy. Data are mean ± SEM. (*) is $P<0.05$.

Table 1

PCR primers

Gene	Sequence	Amplicon Length	Cycles
MMP-2	5’ – agatcttcttcttcaaggaccggtt– 3’ (sense) 5’ – ggctggtcagtggcttggggta– 3’ (antisense)	225	35
MMP-9	5’ – gtttttgatgctattgctgagatcca– 3’ (sense) 5’ – cccacatttgacgtccagagaagaa3’(antisense)	208	35
TIMP-1	5’ – ggcatcctcttgttgctatcactg– 3’ (sense) 5’ – gtcatcttgatctcatcccgctgg– 3’ (antisense)	169	35
TIMP-2	5’ – ctcgctggacgttggaggaaagaa– 3’ (sense) 5’ – agcccatctggtacctgtggttca– 3’ (antisense)	155	35
ADAMTS-1	5’ –cattaacggacaccctgctt– 3’ (sense) 5’ –cgtgggacacacatttcaag– 3’ (antisense)	166	35
18S	5’ –agctaggaataatggaatag-3’ (sense) 5’-aatcaagaacgaaagtcggag- 3’(antisense)	150	19